Materials Science & Engineering A xxx (xxxx) xxx–xxx

Contents lists available at ScienceDirect

Materials Science & Engineering A

journal homepage: www.elsevier.com/locate/msea

Short communication

Deformation mechanism during dynamic loading of an additively manufactured AlSi10Mg_200C

Amir Hadadzadeh[a,b,*], Babak Shalchi Amirkhiz[b], Jian Li[b], Akindele Odeshi[c], Mohsen Mohammadi[a]

[a] Marine Additive Manufacturing Centre of Excellence (MAMCE), University of New Brunswick, Fredericton, NB E3B 5A3, Canada
[b] CanmetMATERIALS, Natural Resources Canada, 183 Longwood Road South, Hamilton, ON L8P 0A5, Canada
[c] Department of Mechanical Engineering, University of Saskatchewan, Saskatoon, SK S7N 5A9, Canada

ARTICLE INFO

Keywords:
Direct metal laser sintering (DMLS)
Transmission electron microscopy (TEM)
Electron backscattering diffraction (EBSD)
Dynamic recovery (DRV)
Dynamic recrystallization (DRX)

ABSTRACT

A DMLS-AlSi10Mg_200C was subjected to dynamic loading at two strain rates. At 1680 s^{-1}, an ultrafine substructure formed inside the α-Al dendrites due to dynamic recovery (DRV). At 4300 s^{-1}, continuous dynamic recrystallization (CDRX) occurred, followed by DRV inside the DRX grains with development of nanoscale subgrains.

1. Introduction

Additive manufacturing (AM) is an incremental layer-on-layer joining process where a three-dimensional part is fabricated from a digital CAD model directly from a powder or wire material feedstock [1]. The feedstock is selectively melted using an energy source which is usually laser, electron beam, electric arc or ultrasonic vibration to create the layers [2–4]. Amongst the available AM processes, selective laser melting (SLM) which is also known as direct metal laser sintering (DMLS) [5] has shown a promising trend for fabricating metallic parts due to its design freedom, shorter production cycle (in comparison to the conventional manufacturing routes), and significant cost savings [6–9]. Moreover, ultrafine, metastable and gradient microstructures formed due to fast solidification rates (10^3–10^6 °C/s) during DMLS process [10]. DMLS has been used widely for processing of aluminum alloy powders [11–14]. In particular, DMLS of AlSi10Mg has received increasing attention due to its light weight, high specific strength, and excellent corrosion resistance [15–17] for applications in aerospace, automotive and marine industries. It has been shown that DMLS-AlSi10Mg parts possess higher strength than the as-cast [18–20] or conventional powder metallurgy [21] counterparts under quasi-static loading conditions. Similarly, under high strain rate loading conditions, DMLS-AlSi10Mg exhibited higher strength than sand cast AlSi10Mg [22]. It is important to investigate the high strain rate deformation of AlSi10Mg alloy since unexpected impact situations in service conditions (e.g. vehicle crash) can expose this alloy to dynamic loading. While dynamic impact loading of conventional metallic alloys leads to formation of adiabatic shear bands (ASBs) and strain localization [23–25], the deformation mechanism during high strain rate deformation of DMLS-AlSi10Mg is not clear yet. Therefore, dynamic loading of a DMLS-AlSi10Mg_200C alloy was investigated in the current study and the deformed microstructure was analyzed using electron backscatter diffraction (EBSD) and transmission electron microscopy (TEM). This study sheds light on high strain rate deformation mechanism, which is used to explain the correlation between microstructure and mechanical behavior of the DMLS-AlSi10Mg_200C alloy.

2. Experimental procedure

AlSi10Mg_200C virgin powder with an average particle size of 9 ± 7 μm and chemical composition of Al-10wt%Si-0.33 wt%Mg-0.55 wt%Fe [20] was used to fabricate vertical rod-shaped samples with 12 mm diameter and 12 cm height using an EOS M290 machine by DMLS technique. The powder particles were fabricated using gas atomization method and possessed spherical or near spherical morphology [20]. The dimensions of the building plate were 250 mm × 250 mm × 325 mm and the machine was equipped with a 400 W Yb-fiber laser and a beam spot size of 100 μm. The building platform was preheated to 200 °C and kept at this temperature to minimize residual stresses. Due to this preheat temperature, this powder is called AlSi10Mg_200C. The laser power, scanning speed, hatching distance, and powder layer thickness was 370 W, 1300 mm/s,

* Corresponding author at: Marine Additive Manufacturing Centre of Excellence (MAMCE), University of New Brunswick, Fredericton, NB E3B 5A3, Canada.
E-mail address: amir.hadadzadeh@unb.ca (A. Hadadzadeh).

https://doi.org/10.1016/j.msea.2018.03.014
Received 22 January 2018; Received in revised form 3 March 2018; Accepted 3 March 2018

190 μm and 30 μm, respectively. An argon atmosphere with an oxygen content of 0.1% was utilized to fabricate the samples. The compressive dynamic shock loading tests were performed using a Split Hopkinson Pressure Bar (SHPB) on cylindrical samples with 9.5 mm diameter and 10.5 mm height along the building direction. Details of shock loading tests set-up can be found in [25]. Microstructure of the as-built sample was analyzed using optical microscopy (OM), scanning electron microscopy (SEM) and EBSD. The EBSD scans were conducted in a field emission gun scanning electron microscope (FEG-SEM) (FEI Nova NanoSEM-650) equipped with an OIM 6.2 EBSD system (EDAX), with a step size of 0.12 μm. To analyze the solidification behavior of the alloy, a computational thermodynamics database, FactSage™ with the FTlite database [26] was utilized. As-built and deformed samples were analyzed using an FEI Tecnai Osiris TEM equipped with a 200 keV X-FEG gun. The Super-EDS X-ray detection system combined with the high current density electron beam in the scanning mode (STEM) was also utilized to analyze the precipitates. Spatial resolutions in the order of 1 nm were obtained during EDS elemental mapping by using a sub-nanometer electron probe.

3. Results and discussion

Fig. 1(a) and (b) show the OM and SEM images of the as-built sample from the side view, where the cross-sections of the melt pools are visible. The overlapped melt pools are almost half-cylindrical in shape [27], which is the typical so-called fish-scale structure in the DMLS-AlSi10Mg parts [28]. Referring to the SEM image of the as-built sample (Fig. 1(b)), the center of the melt pools consists of ultrafine cellular dendritic microstructure with an average size of ~ 0.6 μm. Each cell consisted of α-Al with eutectic Si boundaries. This microstructure has been reported for DMLS of AlSi10Mg in the previous studies [21,29]. At the boundaries of the melt pools, partially melted heat affected zone (HAZ) is observed [30]. Above the HAZ a coarse-elongated columnar structure along the building direction is observed as a result of epitaxial growth [31]. The average cell size in the HAZ and coarse columnar zone is ~ 1.5 μm and ~ 1.03 μm, respectively. Beneath the HAZ, a finer columnar structure is observed with an average cell size of ~ 0.82 μm. Variation of cell size in the microstructure of DMLS-AlSi10Mg_200C is mainly due to the change in thermal gradient during the DMLS process [32]. Fig. 1(c) shows the inverse pole figure (IPF-Z) obtained from EBSD, with detailed information on grain size and orientation. Similar to the cell structure, a heterogeneous grain structure is observed for the material; however, the grain size is at least one order of magnitude larger than the cell size, which is consistent with the previous studies [21]. In other words, each grain is consisted of several cells. The width of the elongated grains can reach ~ 20 μm, while the equiaxed grains at the vicinity of the melt pool boundaries are much finer in size [33]. The majority of the elongated grains developed {100} < 001 > texture which is consistent with the results of previous studies [27,33,34]. Fig. 1(d) illustrates the STEM bright field (STEM-BF) microstructure of the as-built material along with the EDS elemental maps of Al, Si, Mg and Fe superimposed on the image (Fig. 1(e)). The bright areas in the STEM-BF image are primary α-Al phase (shown by green in the map), surrounded by mainly eutectic Si (red in the map). Other intermetallic phases consisted of Mg and Fe are also observed.

The isopleth of Al-0.33 wt%Mg-0.55 wt%Fe-xSi system at Al-rich corner predicted by FactSage™ is shown in Fig. 2(a). The chemical composition of AlSi10Mg_200C used in the current study is shown by a dashed red line on the graph. The possible final phases after solidification of AlSi10Mg_200C include α-Al (primary and eutectic), Si (eutectic), and Al_3FeSi and $Al_8FeMg_3Si_6$ intermetallics. The amount of

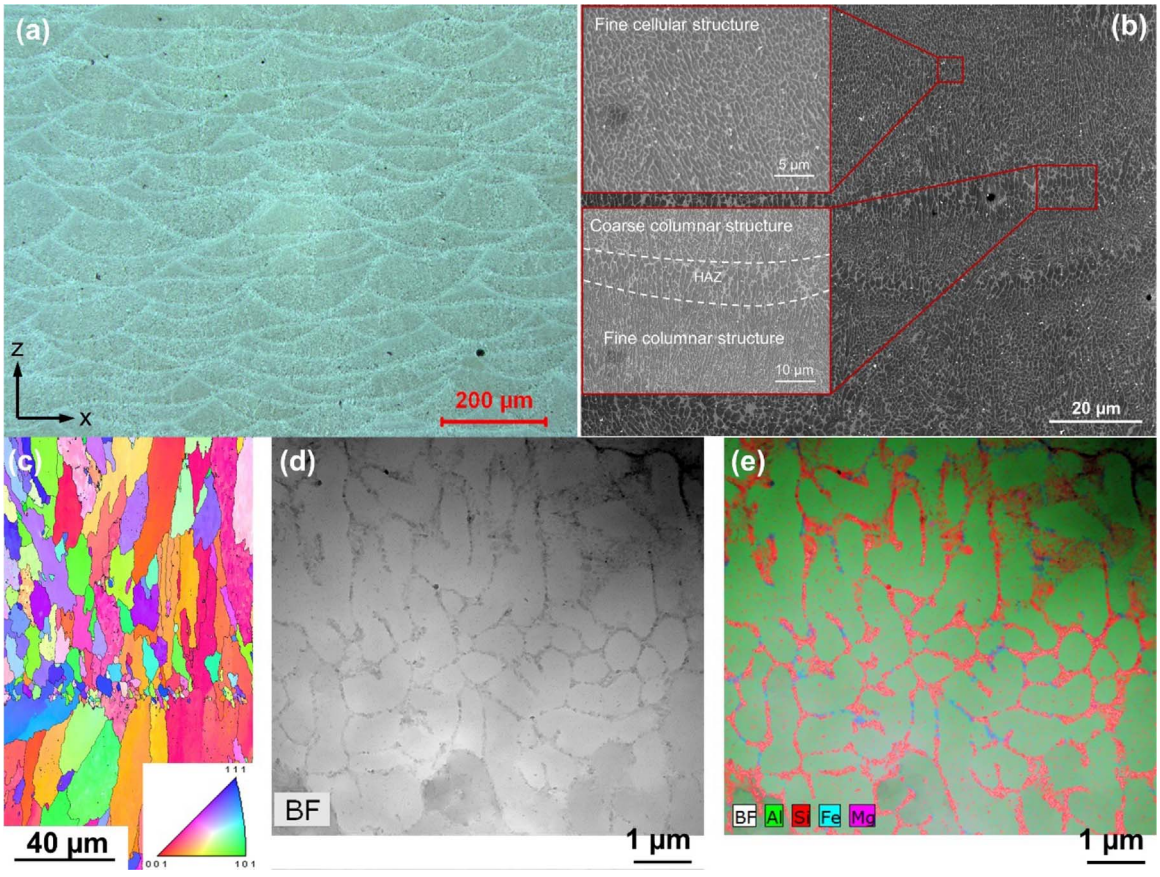

Fig. 1. (a) OM, (b) SEM and (c) inverse pole figure (IPF-Z) images of the as-built AlSi10Mg_200C sample from side view. (d) STEM-BF microstructure of the as-built sample and (e) the corresponding TEM EDS compositional map superimposed on the STEM-BF. z-axis represents the building direction.